Citation: Irzon, R., Syafri, I., Suwarna, N., Hutabarat, J., Sendjaja, P., Setiawan, V.E., 2021. Geochemistry of plutons in central Sumatra and their correlation ti Southeast Asia tectonic history. Geologica Acta, Vol.19.9, 1-14, I-III.
DOI: 10.1344/GeologicaActa2021.19.9

geologica acta

Geochemistry of plutons in central Sumatra and their correlation to Southeast Asia tectonic history

R. Irzon[1] I. Syafri[2] N. Suwarna[3] J. Hutabarat[2] P. Sendjaja[1] V.E. Setiawan[1]

[1]Center for Geological Survey, Ministry of Energy and Mineral Resources
Jl. Diponegoro 57, Bandung, West Java, Indonesia
Irzon E-mail: ronaldoirzon18@gmail.com

[2]Faculty of Geological Engineering, Padjadjan University
Jl. Raya Bandung - Sumedang KM. 21, Sumedang, West Java, Indonesia

[3]Geological Agency, Ministry of Energy and Mineral Resources
Jl. Diponegoro 57, Bandung, West Java, Indonesia

ABSTRACT

Previous investigations of plutons in Sumatra were focused on age dating with minimum geochemistry composition analysis. The purpose of this study is to define the geochemistry classification of the intrusions in central Sumatra on describing the emplacement mechanism associated with Southeast Asia tectonics. The rocks composed of quartz, K-feldspar, and plagioclase with amphibole, biotite, epidote, and zircon as accessory minerals. Six of seven studied plutons range from monzodiorite to granite with metaluminous-slight peraluminous, medium to very high-K calc-alkaline, magnesian, calcic to calc-alkalic affinities. The studied samples depict a wide range of total REE composition of 39-1,369ppm. Most of the rocks denote Sr, Ti, Y, Ce, and Eu anomalies on the primitive-mantle and chondrite normalized diagram. LREE are more enriched in comparison to HREE with $(La/Sm)_N$= 1.71-18.75 and $(Gd/Lu)_N$= 0.15-2.59. Most of the studied plutons are classified in the I-type according to the A/CNK value, negative SiO_2 to P_2O_5 correlation with magnesian and arc-associated character. A-type nature of Sijunjung Granite is displayed on its high silica and REE content with ferroan, calc-alkalic, and within-plate affinities. The existence of A-type intrusion implies an extensional setting during long time subduction episodes, which triggered I-type magmatism since Late Permian to Neogene in Sumatra.

KEYWORDS **Plutons; Central Sumatra; Geochemistry; Tectonics.**

INTRODUCTION

The Southeast Asian region Figure 1 is constituted by continental blocks, namely Indochina-East Malaya, Sibumasu, West Sumatra, West Burma, Southwest Borneo, and Semitau accreted from the Paleozoic to the end of Mesozoic (*i.e.* Barber and Crow, 2009; Breitfeld *et al.,* 2017; Hall and Sevastjanova, 2012; Hazad *et al.,* 2019; Hutchinson, 2014; Metcalfe 2011, 2013; Ng *et al.,* 2017). Cathaysia block including Indochina-East Malaya,

West Sumatra, and West Burma, was added to Eurasia since the Palaeozoic while Sibumasu was accreted in the Triassic. Southwest Borneo Block and the small Semitau terrane accreted during the Late Cretaceous (Metcalfe, 2011, 2013). The West Burma block in Myanmar and West Sumatra have been separated by the development of the Andaman Sea since the Miocene (Barber and Crow, 2009; Hutchinson, 2014; Metcalfe, 2011). The Bentong Raub Suture represents the closure of the Palaeo-Tethys and marks the boundary between Sibumasu and Indochina in Indonesia, whereas the Median Sumatra Tectonic Zone separates the West Sumatra from Sibumasu (Barber and Crow, 2009; Hall and Sevastjanova, 2012; Metcalfe, 2011; Ng *et al.,* 2017). The Boyan Suture is the boundary between the Southwest Borneo and the small Semitau in northern Borneo. Three Tethyan oceans were involved in the development of the Southeast Asia terranes, namely, the Devonian-Triassic Palaeo-Tethys, the Early Permian-Late Cretaceous Meso-Tethys, and the Late Triassic-Late Cretaceous Ceno-Tethys (Jiang *et al.,* 2017; Hutchinson, 2014; Metcalfe, 2013). The subduction of the Indian Plate beneath Asia was considered to have initiated in the Eocene (Ali and Aitchison, 2005; Irzon *et al.,* 2018; Setiawan *et al.,* 2017).

The long-term continent-continent and ocean-continent convergence in Southeast Asia led to plutonism and the development of both fore-arc and back-arc basins (Hutchinson, 2014; Metcalfe 2011, 2013). The three igneous provinces in Southeast Asia, specifically, Eastern, Main and Western ranges are associated with the above-mentioned convergent settings. The subduction of the Palaeo-Tethys Ocean below Indochina-East Malaya

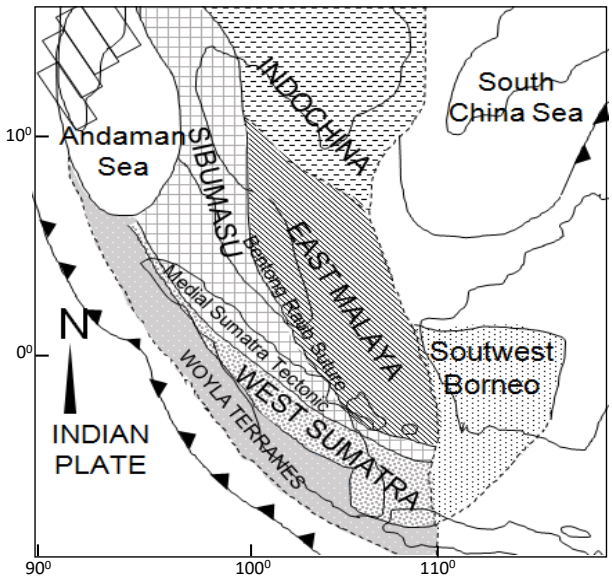

FIGURE 1. Present tectonic plates in Southeast Asia terrane (modification after Metcalfe (2011)).

triggered the development of the Eastern granite province whilst the later collision of Sibumasu and Indochina-East Malaya generated the Main Range province (Barber *et al.,* 2005; Gasparon and Varne, 1995; Irzon *et al.,* 2020; Metcalfe, 2013; Ng *et al.,* 2017). Within the Malay Peninsula, the Eastern province was further subdivided into the Central and Eastern Belts while Main Range Belt corresponds to the Main Range province (Cottam *et al.,* 2013; Nguyen *et al.,* 2019). Ceno-Tethys subduction-related Western Province extends mainly from Upper Peninsula Thailand into Myanmar (*i.e.* Hazad *et al.,* 2019; Jiang *et al.,* 2017). In addition, Clark and Beddoe-Stephens (1987) proposed to include the Hatapang Granite in northern Sumatra as a part of the Western Province, on the basis of its geochemical affinities. Based on the investigation along the suture between Mergui Microplate and the Permian Volcanic arc in Central Sumatra, another granitic belt was identified (McCourt *et al.,* 1996). The subduction-related magmatism formed small batholiths emplaced nearby the continental margin of Sundaland to the southwest on West Sumatra, which was amalgamated to Sibumasu in the Early Triassic (McCourt *et al.,* 1996). Other studies interpreted these plutons as a volcanic arc suite nearby the Bukit Barisan Mountains with composition ranging from gabbro to monzogranite (Cobbing, 2005; Irzon *et al.,* 2018).

Small intrusions in the central Sumatra are mostly emplaced in the volcanic arc suite. The oldest pluton is the Ombilin Granite (OG), which was dated at 277-246Ma (Koning and Aulia, 1985 in Barber *et al.,* 2005; Suwarna, 2000 in Barber *et al.,* 2005). K-Ar in biotites from Sijunjung Granite (SG) yielded the Late Permian Age while the Sulit Air Granite (SAG) yielded the Triassic to Jurassic ages (McCourt and Cobbing, 1993 in Barber *et al.,* 2005; Sato, 1991). The studies on the Tanjung Gadang Granite (TGG) resulted in a Late Jurassic to Early Cretaceous age applying the Rb-Sr method (Koning and Aulia, 1985 in Barber *et al.,* 2005; Pulonggono and Cameron, 1984). Three other intrusives, namely Padang Panjang Pluton (PPP), Lassi Pluton (LaP) and Lolo Pluton (LoP) were emplaced during Paleocene, Eocene, and Miocene, respectively (McCourt and Cobbing, 1993 in Barber *et al.,* 2005; Sato, 1991). However, these previous studies were focused on age dating with incomplete trace and rare earth elements (REE) analysis (*e.g.* Imtihanah, 2005; Sato, 1991).

Most of the Mesozoic intrusions in Sumatra are I-type, subduction-associated, and situated in the Barisan Mountains (Barber, 2000; McCourt *et al.,* 1996; Zhang *et al.,* 2018). However, several studies notified the presence of anorogenic A-type intrusions, namely Sibolga Granite (Setiawan *et al.,* 2017; Zhang *et al.,* 2020) and Sijunjung Granite (Irzon *et al.,* 2018) in the central Sumatra region. Therefore, more complete petrography and geochemistry data on these plutons are required to explain the tectonic

history of Sumatra. The aim of this paper is to establish the classification of plutons from central Sumatra on drawing their correlation with Southeast Asia tectonic history.

Geological Setting

Sumatra is situated at the western edge of Indonesian archipelago and at the northeastern margin of Indian Ocean. The island is presently constituted of two major continental blocks: the Cathaysian West Sumatra and the northern Gondwana-origin Sibumasu. Cathaysia which is formerly consisted of Indochina, South China, North Qiantang-Qamdao-Simao, West Burma, and West Sumatra, possibly began to move away from Gondwana during Devonian across the Palaeo-Tethys Ocean (Barber and Crow, 2009; Hall and Sevasjanova, 2012; Metcalfe, 2011, 2013). West Sumatra and West Burma detached from the Cathaysia since Permian and inserted at the west margin of Sibumasu during Triassic (Barber *et al.*, 2005; Barber and Crow, 2009). The two blocks were separated by the Andaman Sea since the Miocene. The contact of the West Sumatra and the Sibumasu blocks is marked by the Medial Sumatra Tectonic Zone (MSTZ), which extends from the Andaman Sea to southern Sumatra (Barber and Crow, 2009). The studied intrusions are situated in a volcanic arc suite on the West Sumatra continental region (Figure 2). The plutonic rocks are located in the proximity of the volcanic Bukit Barisan Mountains, which extends almost 1,700km from north to South of Sumatra.

Volcanic rocks were emplaced in Sumatra episodically since pre-Triassic. Silungkang and Palepat Formations are the two Permian extrusive rock units located in central Sumatra region. The Palepat Formation which comprises basic to intermediate lava lies near Tanjung Gadang while the Silungkang Formation that is situated to the southeast of Lake Singkarak and at the north of Ombilin Granite mainly consists of andesite and meta-andesite (Silitonga and Kastowo, 1995). Most of the Tertiary volcanic rocks in Central Sumatra are situated less than 10km before the west coast of Sumatra. Quaternary extrusives that occupy large area in the studied location are easily found near mountains, lakes, and sometimes near pluton bodies (Figure 2). Metamorphic rocks in Sumatra generally resulted from contact effect of intrusion and subsequently by shearing (Barber and Crow, 2009).

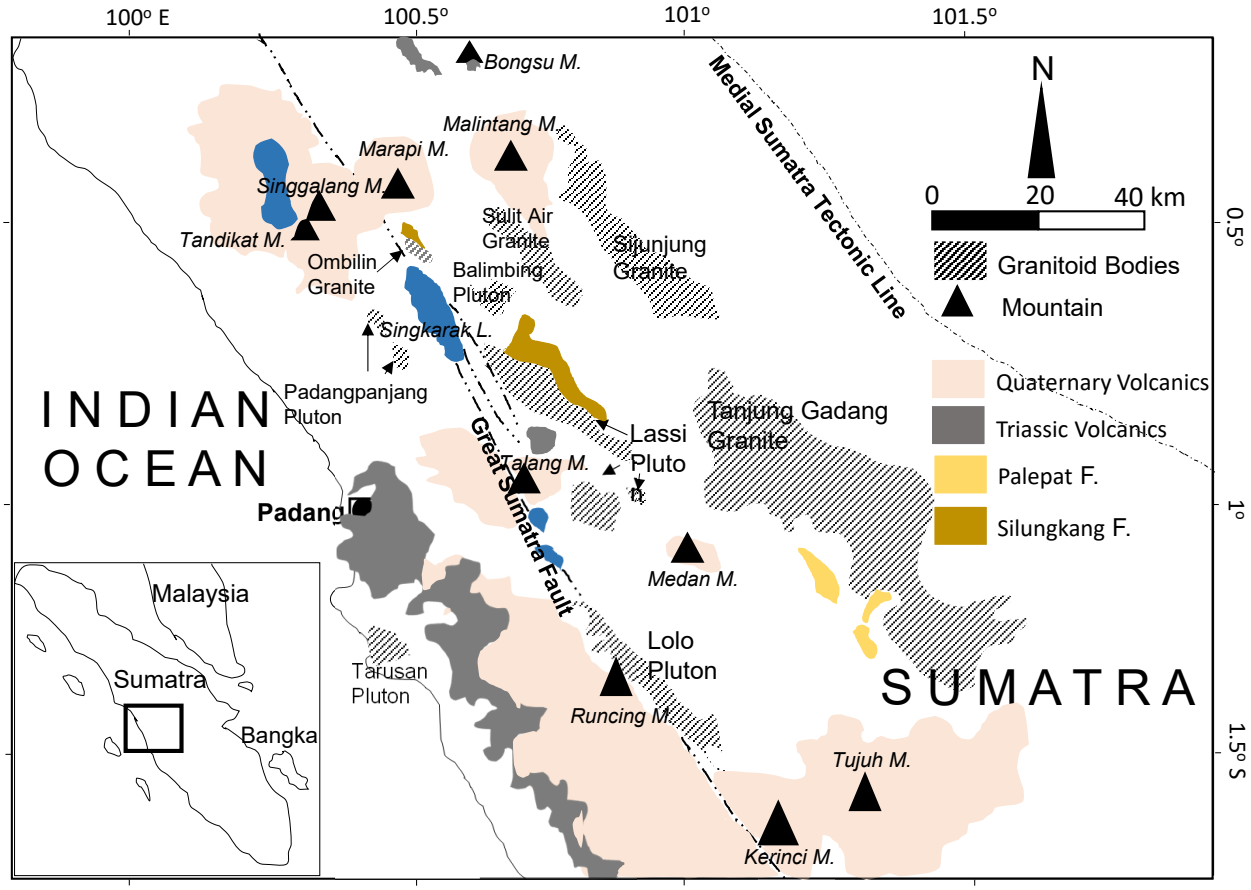

FIGURE 2. Studied plutons situated in the west of Medial Sumatra Tectonic Line on the West Sumatra block (modified after Cobbing, 2005). Mountains in the western region of Sumatra form the Bukit Barisan Mountains.

SAMPLE DESCRIPTIONS

Sijunjung Granite

The Triassic Sijunjung Granite (SG) is exposed in the northern part of the studied region with a dimension of about 50×10km^2 (Silitonga and Kastowo, 1995) as shown in Figure 2. Major geochemistry composition of two samples from this pluton were provided by Sato (1991) and Sutanto (2005). The pluton was crystallized in the Triassic according to K-Ar biotite and hornblende datings (Sato, 1991; Silitonga and Kastowo, 1995). This study analyzed five SG samples (SJ-30, SJ-31, SJ-87, SJ-89 and SJ 90). SJ-30 and SJ-31 were collected from the northwest whilst the others from the south of the granite body. The specimens are fresh, pinkish, coarse-grained, porphyritic with a mineral assemblage formed by quartz, K-feldspars (megacrystal), biotite, and plagioclase. Hornblends are clearly detected in a couple of samples from the south of this intrusion.

Balimbing Pluton

The 16km^2 Balimbing Pluton is situated to the east of Singkarak Lake (Figure 2). OB-26 and OB-27 are the fresh light grey and medium-grained rocks of Balimbing Pluton (BP). Some very fine-grained aplites were identified at the OB-26 outcrop. The samples are mainly composed of quartz, K-feldspar, biotite, and hornblende.

Sulit Air Granite

The Triassic Sulit Air Granitoid (SAG) is located to the east of the Balimbing Pluton and to the southwest of the Sijunjung Granite. Cu mineralization is detected in the 60km^2 pluton. Imtihanah (2005) described major geochemistry of two samples from SAG. This study collected four more samples from the pluton: SA-34, SA-54, SA-56 A and SA-56 B. The first two are relatively unaltered, light grey, and medium-grained rocks. SA-56 A is a dull, medium-grained, and chloritized intrusion while SA-56 B is a malachite ore with high Cu composition.

Tanjung Gadang Granite

The 60x35km^2 large Cretaceous Tanjung Gadang Granite (TGG) body is placed to the southwest from SG and to the west from Lassi Pluton (LaP). Intrusive rocks with their weathering horizons were found at TG-02 and TG-05 stations on Tanjung Gadang Granite domain. TG-02 might have been influenced by a higher degree of weathering than TG-05 regarding its colour. The specimens are majorly built of quartz, plagioclase, K-feldspar with minor biotite.

Lassi Pluton

The Lassi Pluton (LaP) crops out in three different bodies (Figure 2) with a northwest elongate exposure of about 38x9km^2. Sato (1991), Imtihanah (2005) and Sutanto (2005) discussed a total of six samples of the Eocene pluton regarding its petrography and major geochemistry points of view. Ten LaP rocks are described and are analyzed in this paper. LS-06, LS-07 A, LS-07 B, LS-08, LS-15 and LS-16 were sampled from the northern body of Lassi Pluton whilst LS-12, LS-20 and LS-62 from the southwestern ones. Six of the samples are categorized as fresh, light grey, medium-grained rocks whilst LS-06, LS-07 A, LS-07 B, LS-08 and LS-15 might have experienced some degree of alteration regarding foliations, color, and texture. The alteration might be explained by their location close to the Great Sumatra Fault (Figure 2).

Lolo Pluton

Alike the northern part of LaP, the Miocene Lolo pluton (LoP) is also emplaced just near the Great Sumatra Fault and to the west of Mount Runcing (Figure 2). Imtihanah (2005) analyzed four samples from the 45km^2 pluton geochemically but with incomplete REE composition. This work investigated new three samples of LoP, namely LL-58 A, LL-58 B and LL-59. The rocks are light grey, medium grain, and relatively fresh with hornblende crystals detected megascopically. LL-58 might be located towards the edge of the intrusion because hornfels were also discovered near the sample location.

Tarusan Pluton

The Tarusan Pluton (TP) is located near the west coast of Sumatra about 20km to the south from Padang. No previous investigation ever discussed on the approximately 8km^2 rock body. Two samples were attained from this location, namely TR-35 A and TR-35 B. TR-35 A is a pinkish, phaneritic, coarse grain, and massive rock whereas TR-35 B is relatively more brownish because of weathering. Both of the specimens are composed of quartz, K-feldspar, and plagioclase without hornblende observed.

Petrographic Characteristics

The selected plutonic rocks are generally medium to coarse grain, having a porphyritic texture, and poor alteration tendency. Quartz (0.1-1.5mm) is the most predominant mineral in the range of 28-46% modal composition. The euhedral and transparent phase form interlocking texture is detected in a few samples. Although most of the quartz show well-developed crystal faces, some of them have round embayments. The selected samples are built of 7-21% modal composition transparent plagioclase. Some

of the subhedral minerals are characterized by albite and Carlsbad-albite twinning. Alkali feldspar of the samples is subhedral and transparent in the range of 5-24% modal composition. Except for the SG and TP, hornblende and biotite are found in most of the microscopic analysis (3-15 modal %). Some plagioclase and alkali feldspar are weakly altered to sericite as shown in LL-59 from LoP. Some of the biotite and plagioclase grains are to chlorite and epidote.

SG is special for the presence of alkali feldspar megacrystals. Some K-feldspars are covered by plagioclase with rapakivi texture. Mica muscovite (5-7 modal %) and zircon are only detected in this Triassic intrusion. Muscovite rarely occurs as separate crystal associated with biotite and some is also identified in feldspar as secondary inclusions. In SG samples, very fine grain zircon and apatite show euhedral to subhedral crystals and commonly as inclusion in quartz. The modal microscopic analysis results of selected rocks are given in Table 1. In the QAP ternary plot, the LaP, LoP, TP and SG samples fall within monzogranite-granodiorite, granodiorite, syenogranite-monzogranite, and syenogranite fields, respectively (Figure 3).

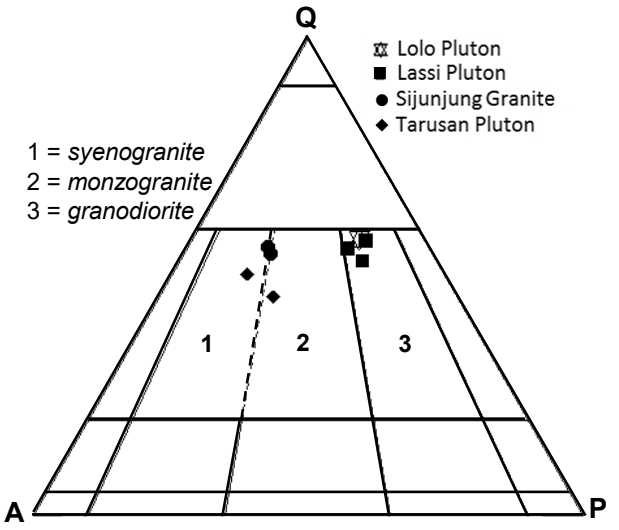

FIGURE 3. Quartz–Alkali feldspar–Plagioclase (QAP) plot (after Streckeisen, 1976) of selected samples from central Sumatra plutons. The selected rocks plotted in quartz-rich granitoid (2 samples), syenogranite (4 samples), monzogranite (1 sample), and granodiorite (2 samples) fields.

ANALYTICAL METHODS

Major oxides analysis of 29 samples was conducted using Advant X-ray fluorescence (XRF) while trace elements and the full suite rare earth elements compositions were measured using the quadrupole X-Series Thermo Inductively coupled plasma-mass spectrometry (ICP-MS). Both geochemistry preparation and analysis were performed in the Center for Geological Survey Laboratory in Bandung. Loss on ignition (LOI) measurements were carried out by heating the samples at 1000°C for an hour to determine their relative weight loss. AGV-2, GBW 7110 and GBW 7113 were the certified reference materials used in this study in verifying measurement accuracy. The detail of the preparation procedure, the analytical instrument setting, and data verification protocols followed the previous studies of Irzon (2017) and Irzon (2018). Data from previous studies are also incorporated in this paper. Whole rock geochemical composition of this study is shown in Table I, Appendix I.

RESULTS

Major Elements Classification

Some of the studied samples are altered based on the LOI values >2%, so their composition has been recalculated to 100% before plotting in geochemistry-based diagrams. According to the major oxides classification of Middlemost (1994), the samples plot in the monzodiorite (1 sample), diorite (7 samples), granodiorite (3 samples), the granite (9 samples) fields as shown in Figure 4A. The high felsic character ($SiO_2 \geq 70\%$) is denoted on SG, TP and TG Granite.

TABLE 1. Modal composition of microscopict analysis on plutons in Central Sumatra (%)

Sample	Pluton	Primary min.						Accessory			Secondary			Opaque min.
		Qtz	Kfs	Plg	Bt	Ms	Hb	Px	Zr	Apt	Ser	Chl	Ep	
LS-16	LS	35		20	2		10	10				8		15
LS-62	LS	38	10	20	8		12					7		5
LS-63	LS	37	5	20	10		15				5	5	3	
SJ-30	SJ	28	15	8	10	6	5		5	2	7	6	3	5
SJ-31	SJ	27	14	7	12	7	3		10		7	5	5	8
SJ-87	SJ	27	14	7	7	5	5		10	5	5	5	5	5
TR-35	TR	33	24	15						12	8			8
TR 35-	TR	37	26	10						18	2	2		5
LL-59	LL	46	6	21	8		5				5	4		5

The Alumina Saturation Index (ASI) or molar A/CNK (Al_2O_{23}/CaO+Na_2O+K_2O) of the plutons from central Sumatra are mostly <1.1. SAP, TP and LoP are clearly metaluminous with the molar A/CNK <1 (Figure 4B). On the other hand, the SG and LaP are in metaluminous to slight peraluminous array. The peraluminous character of some samples might result from partial melting of metasedimentary rocks and mafic source rocks or amphibolites (Chappel *et al.,* 2012; Nguyen *et al.,* 2019; Sarjoughian and Kananian, 2017).

The intrusions from central Sumatra show markedly different array as seen in the SiO_2 versus K_2O chart. LoP, LaP, SAG, and BP show calc-alkaline to high-K calc-alkaline tendency whereas TP and TGG are high-K calc-alkaline. SG depicts the richest potassium which is classified in Shohonite Series (Figure 5A). Moreover, the SG is ferroan with high Fe* (FeO_T/(FeO_T+MgO)) values (Figure 5B) which implies strong iron enrichment than the other magnesian plutons. On the basis of Modified Akaline-Lime Index (MALI), both ferroan and magnesian rocks can be further classified into calcic, calc-alkalic, alkali-calcic and alkalic. The SG samples fall in alkali-calcic and alkalic fields whereas the others mostly range in calcic and calc-alkaline (Figure 5C).

Trace and Rare Earth Elements Characters

Total REE content in the studied rocks is in the range of 39ppm (LS-16, LaP) to 1,369ppm (SJ-30, SG). SG rocks show higher Ga, Rb, Y and Ba, but lower Sc concentration relative to the other six intrusions. Moreover, this Triassic pluton has the highest REE content of averagely 466 ppm. The normalized trace elements in most studied rock suites, display comparable distribution patterns with negative anomalies for Sr, Ti and Y (Figure 6). However, the rocks from TP denote positive Y anomaly while the southern group of LaP without Y anomaly. Sr and Ti negative anomalies should have been generated from plagioclase and titanite removal, respectively (Perez-Soba and Villaseca, 2010; Sarjoughian and Kananian, 2017).

The chondrite-normalized REE patterns depict the more light-REE (LREE) enrichment ($(La/Sm)_N$ = 1.71-18.75) in comparison to heavy-REE (HREE, $(Gd/Lu)_N$= 0.15-2.59). Steeper negative slope on REE pattern is represented in SG and the northern rocks from LaP, for which the average value of $(La/Yb)_N$ is 8.41 and 9.87, respectively. Most of the studied plutons generally exhibit negative Ce anomaly (Ce/Ce*= 0.01-0.85), except for a couple of rocks from Sijunjung Granite and a Tarusan Pluton sample without notable Ce anomaly. Negative Eu anomaly which indicates plagioclase fractionation (*i.e.* Elitok *et al.,* 2014; Irzon and Abdullah, 2016; Irzon, 2017; Kara *et al.,* 2018; Montez *et al.,* 2017) is shown by most of the samples in the range of 0.13 to 0.84 and emphasized the previous Sr anomaly. On the other hand, rocks from the northern part of LaP display positive Eu anomaly to emphasize different evolution process.

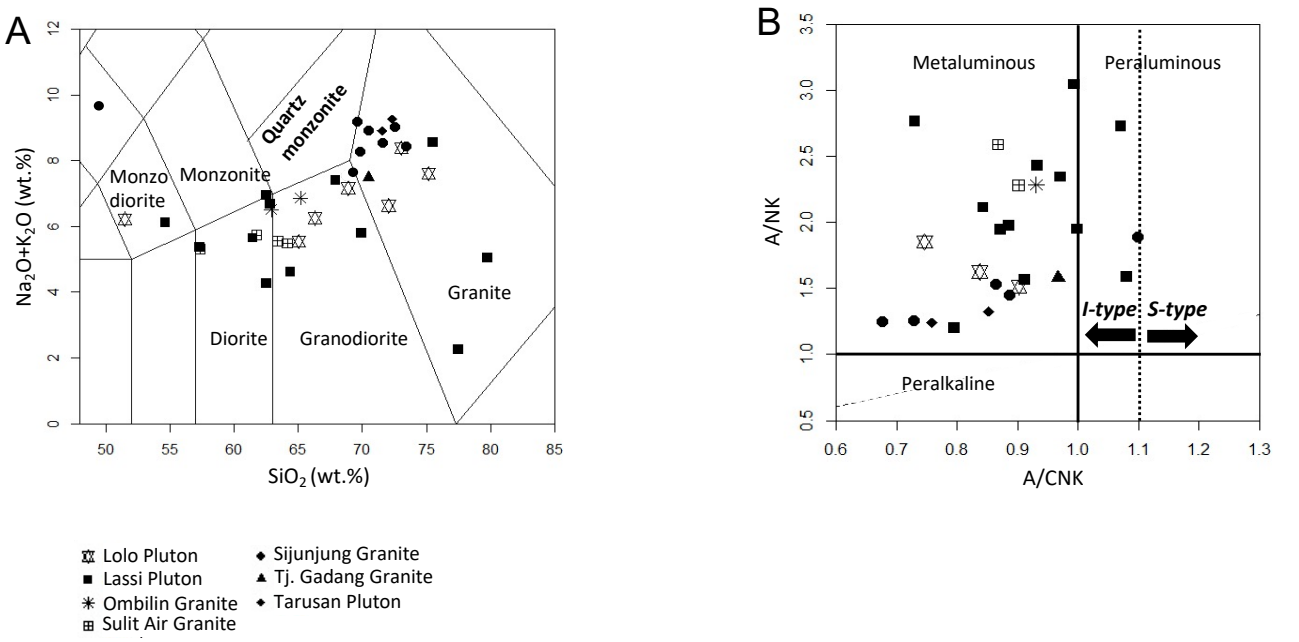

FIGURE 4. A) The plutons in Central Sumatra show a wide range on Total Alkali-Silica (TAS) diagram (after Middlemost, 1994) from monzodiorite to granite. However, Sijunjung Granite depicts the most felsic character and fall within granite field; B) Most of the samples are metaluminous except LS-16 (Lassi Pluton) and SB-89 (Sijunjung Granite) on the A/CNK (molar Al_2O_3/(CaO+Na_2O+K_2O)) versus A/NK (molar Al_2O_3/(Na_2O + K_2O)) diagram (after Maniar and Piccoli, 1989).

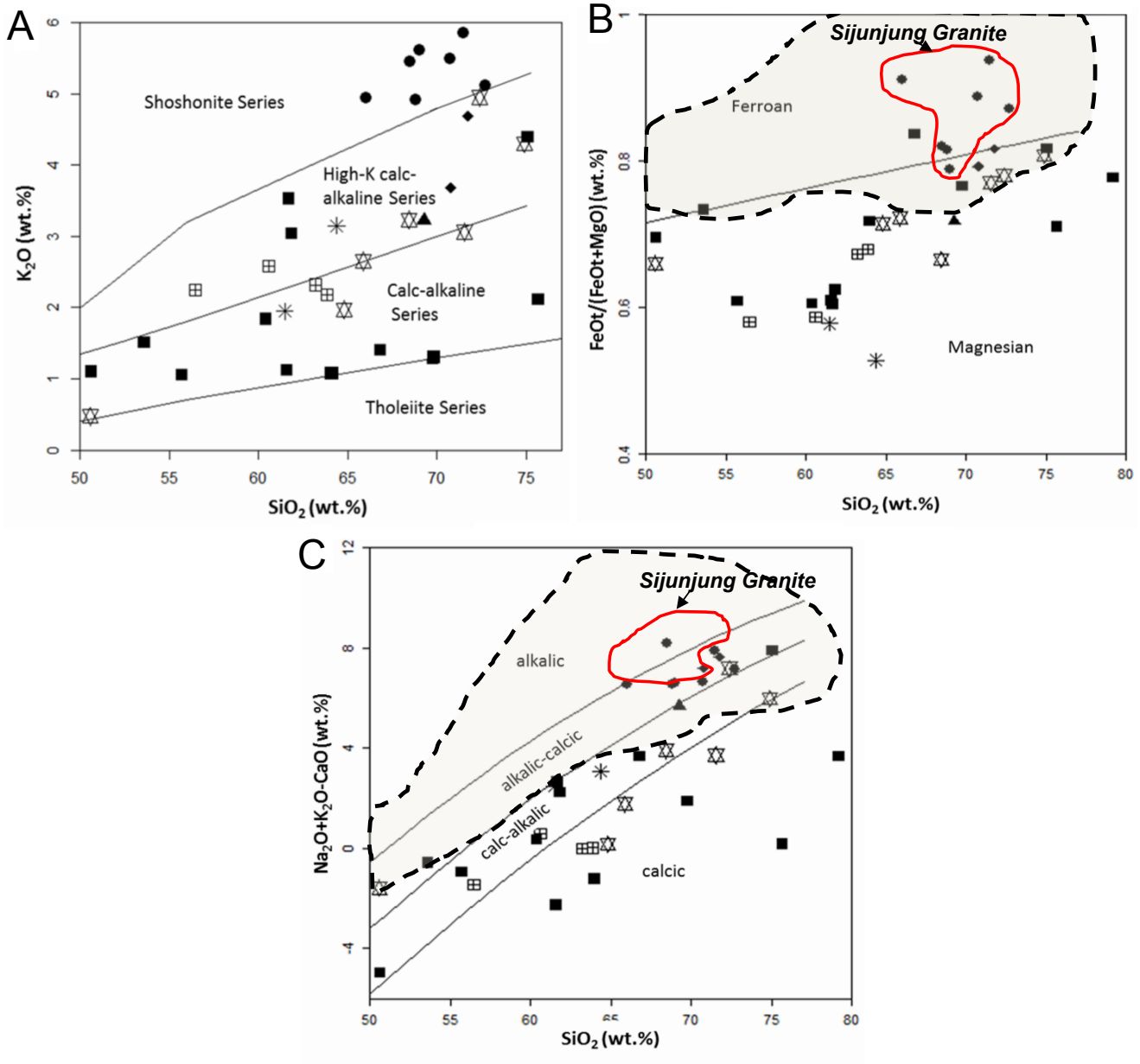

FIGURE 5. SG indicate different natures with other studied plutons: A) identified as Shoshonite series in SiO_2 versus K_2O diagram (after Peccerillo and Taylor diagram, 1976); B) classified in ferroan field (after Frost *et al.*, 2001) and C) shows alkali-calcic to alkalic character. Symbols are the same as Figure 4.

Negative Ce anomaly in igneous rocks explains that the source material exposed just below the surface or as a result of post-magmatic supergene processes under oxidizing conditions (*i.e.* Gazel *et al.*, 2006; Lee *et al.*, 2013). The strong positive correlation of Ce anomaly to Eu anomaly on SG, the northern group of LaP and LoP with correlation coefficient of 0.81, 0.86, 0.98, respectively might imply a secondary oxidizing conditions after emplacement, rather than their nature during magmatic differentiation. However, the number of samples from the other plutons is not enough to establish such conclusion.

DISCUSSION

Alphabetic Classification

The most commonly used plutonic rocks classification is the alphabetic-SIAM scheme. The igneous (I-type) and supracrustal (S-types) granites were proposed based on the research in Lachland Fold Belt (Chappel and White, 1974). The anorogenic or rift-related A-type rock was originally explained by Loiselle and Wones (1979) whereas the description of the subducted oceanic crust derived

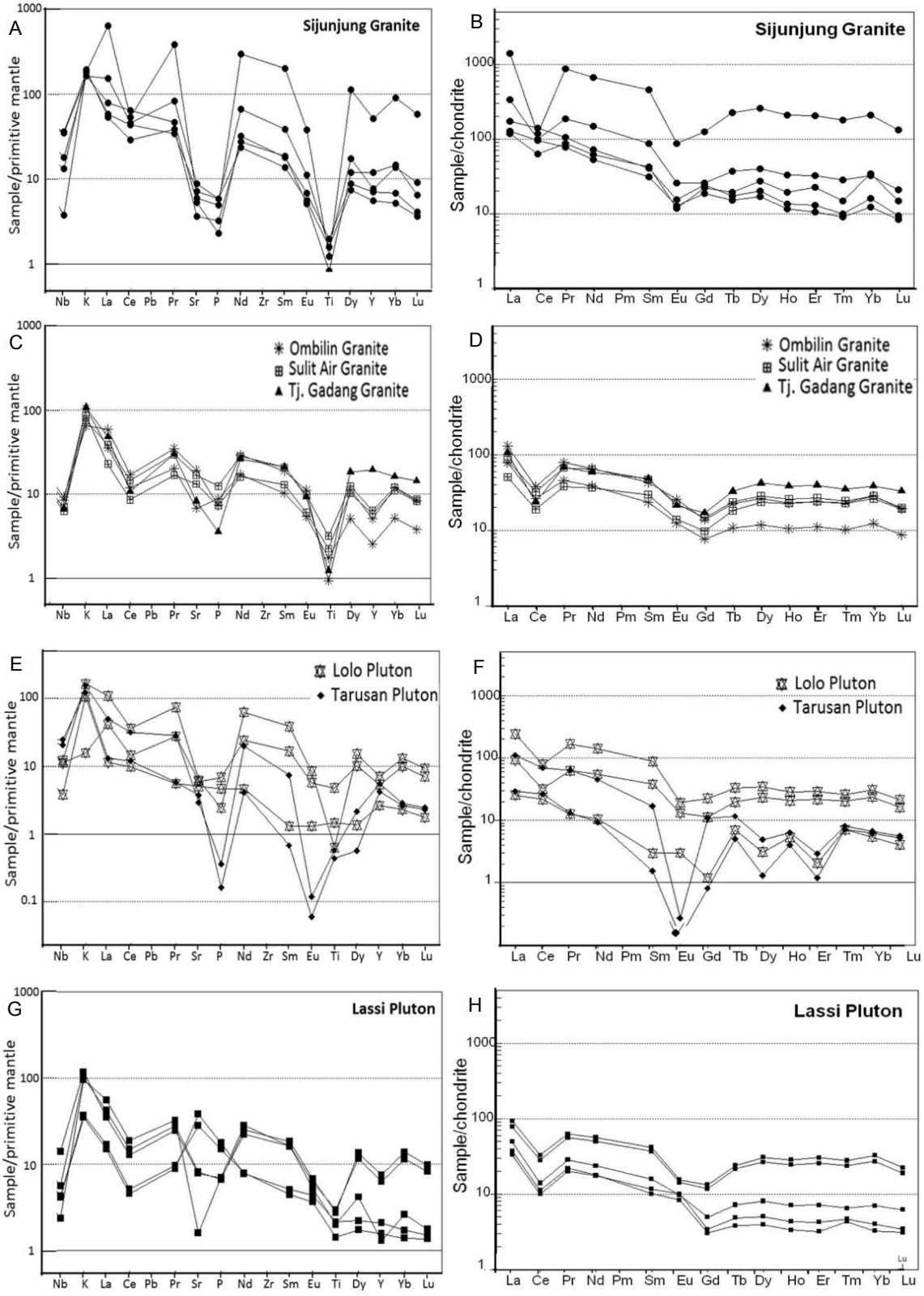

FIGURE 6. Primitive mantle (Sun and McDonough, 1989)-normalized trace element variation and chondrite (Boynton, 1984)-normalized REE variation diagrams for the plutons in Central Sumatra: A, B) The high REE content Sijunjung Granite; C, D) A relatively similar pattern on Balimbing Granite, Sulit Air Granite and Tanjung Gadang Granite; E, F) three samples from Lolo Pluton and a deep Eu negative anomaly at Tarusan Pluton and G, H) Lassi Pluton which depicts two different characters.

M-type intrusion was suggested by Whalen (1987). The classification of this alphabetic scheme was determined on both minerals and geochemistry characteristics.

The predominance of hornblende and biotite combined with a lack of muscovite and monazite minerals is a feature of I-type intrusive rocks (*i.e.* Irzon *et al.,* 2020; Sarjoughian and Kananian, 2017). It is generally accepted that I-type pluton is metaluminous to slight peraluminous with A/CNK<1.1 whilst S-type granites is characterized by a strong peraluminous affinity (*i.e.* Charusiri *et al.,* 1993; Irzon, 2016; Irzon *et al.,* 2020; Nguyen *et al.,* 2019). In several cases, peraluminous nature could also result from highly fractionated I-type granites (Jamil *et al.,* 2016; Perez-Soba and Villaseca, 2010; Pollard *et al.,* 1995). SiO_2 to P_2O_5 correlation is useful for distinguishing the I- and S-type granite, in which I-type granites show a negative correlation while S-type rocks show a positive one (*i.e.* Ghani *et al.,* 2013; Nguyen *et al.,* 2019). The most unique feature of I-type granites is the magnesian composition whatever their affinity to Peacock index series, namely calcic, calc-alkalic, alkali-calcic and alkalic (Castro, 2019). Most plutons in central Sumatra are classified as I-type based on the metaluminous to slight peraluminous and magnesian features with negative SiO_2-P_2O_5 correlation. Moreover, these plutons fall within Volcanic Arc Granites (VAG) field on the Y+Nb versus Rb and Y versus Nb plots (Figure 7).

SG denotes different characteristics with the other studied plutons in this paper. The Al_2O_3 and CaO contents of the Triassic intrusion is low but with high SiO_2, Nb, Na_2O+K_2O, and total REE abundances (Table II, Appendix I) as the indications of A-type granite (Loiselle & Wones, 1979; White & Chappell, 1983). Those characters combined with the distinctly high TiO_2/MgO and K_2O/Na_2O ratios (Figure 8) imply shallow crust origin of the rock (Patiño Douce, 1997). The ferroan, calc-alkalic, metaluminous-peraluminous, and high-silica content (SiO_2≥70%) of Sijunjung Granite is coeval with the A-type plutons widespread in Burma (Jiang *et al.,* 2017), Namibia (Stammeier *et al.,* 2015), southwestern United States and Amazonia (Frost and Frost, 2011). Frost *et al.* (2016) argued that this kind of silica-rich intrusion results from partial melting of tonalite or granodiorite. In the tectonic discriminant diagram of Pearce *et al.* (1984), the Sijunjung Granite tends to be in the field of the A-type within-plate granites (Figure 7).

Tectonic Implication

Studies explain that I-type magmatism is generally triggered by subduction in an active continental margin of igneous derived material while S-type is mostly emplaced in continental collisional and intraplate orogenies because of crustal thickening causing melting of lower crustal metasedimentary rocks (*i.e.* Jiang *et al.,* 2017; Liu *et al.,* 2020; Oliver *et al.,* 2014; Sarjoughian and Kananian, 2017; Setiawan *et al.,* 2017). Castro (2019) argued that a fluid-fluxed melting of igneous rocks in the continental crust in short time span (<30Myr) also generates secondary I-type granites and is not directly associated with a subduction setting. The later mechanism of I-type intrusion is not common in Southeast Asia due to the presence of long

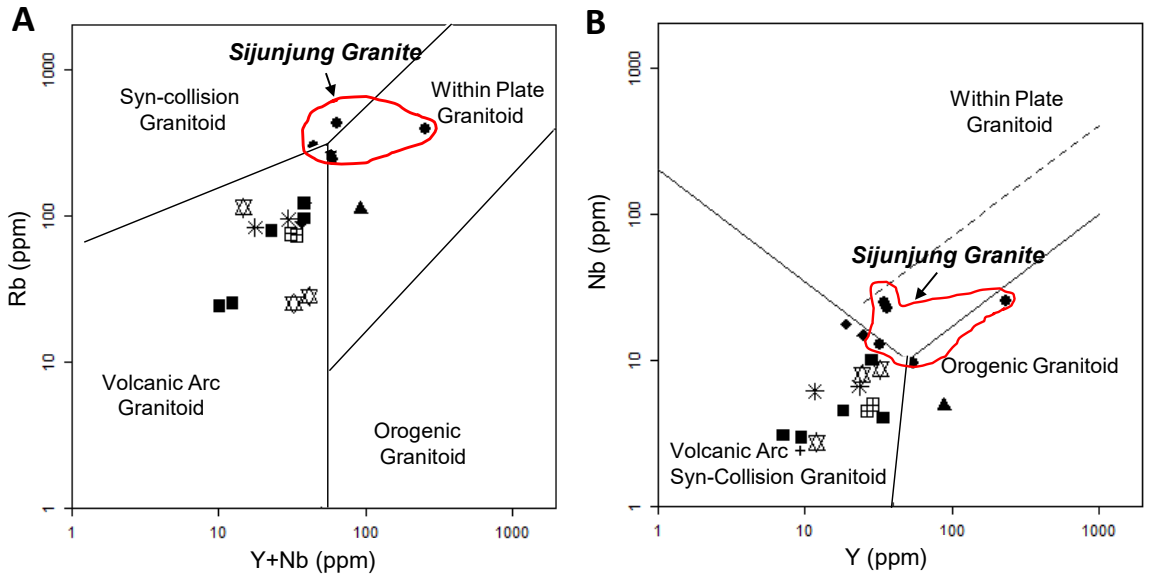

FIGURE 7. The samples of Sijunjung Granite typically fall within the within-plate granite field of Pearce *et al.* (1984) discrimination to imply the A-type character on A) (Y+Nb) versus Rb; and B) Y versus Nb diagrams.

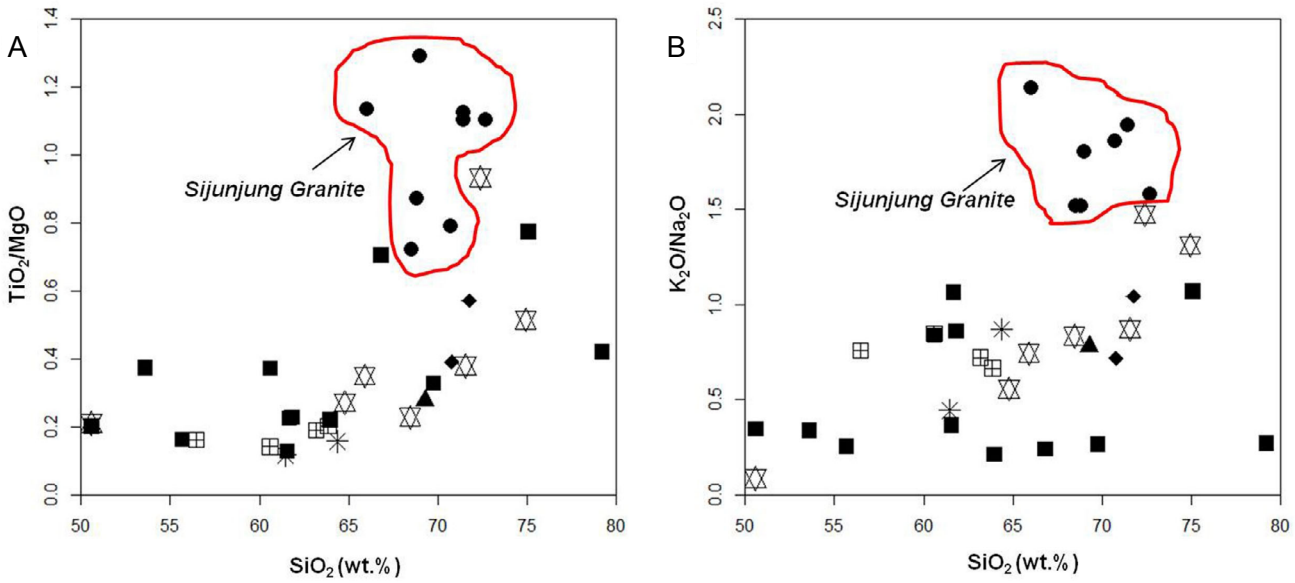

FIGURE 8. A) SiO_2 versus TiO_2/MgO ration and B) SiO_2 versus K_2O/Na_2O ratio of the studied rocks. Sijunjung Granite denotes higher TiO_2/MgO and K_2O/Na_2O ratios than other intrusions.

life subduction both below Indochina-East Malaya resulting the Eastern Province (Late Permian-Triassic) and beneath West Burma-West Sumatra that generated the Western Province (Triassic-Miocene). In most cases, A-type granite is emplaced in extensional tectonic environments and do not appear to be associated with plate boundaries (Amiruddin, 2011; Searle *et al.,* 2012; Setiawan *et al.,* 2017). Recent Sumatra is formed after a long period of plates detachment, rotation, and accretion/amalgamation involving continent-ocean and continent-continent convergencies in Southeast Asia region. Long term intrusions in Sumatra are evidenced from the Late Permian Ombilin Granite to the Miocene Lolo Pluton (Barber *et al.,* 2005). Almost all of the studied plutons are categorized as arc-associated I-type intrusions except for the Sijunjung Granite with anorogenic A-type characteristics as discussed above. The presence of the A-type intrusion explains an extension setting during long time subduction episodes in Sumatra that also happened in Sibolga (Setiawan *et al.,* 2017; Zhang *et al.,* 2020).

Palaeo-Tethys was opened during the Permian at the time when the composite Cathaysia separated from Gondwana. The subduction of the ancient ocean below Indochina should have begun in the Permian (Hutchinson, 2014; Metcalfe, 2013). Meanwhile, some part of Cathaysia, especially West Sumatra and West Burma drifted away since the Late Permian. The Late Permian OG (Koning and Aulia, 1985 in Barber *et al.,* 2005; Silitonga and Kastowo, 1995) most possibly intruded before West Sumatra and West Burma separated from Cathaysia. Sibumasu started to drift away from Gondwana since the Early Triassic that opened the Meso-Tethys but narrowed the Palaeo-Tethys (Metcalfe, 2011). On the other side, West Sumatra and West Burma rotation finished and the plates accreted to Sibumasu. No convergency happened during that time to postulate the anarogenic origin of the Late Permian-Early Triassic SG (Sato, 1991; Silitonga and Kastowo, 1995). The crystallization of SG is coeval with Sibolga Granite, which also indicates several anarogenic facies (Setiawan *et al.,* 2017). The Palaeo-Tethys totally closed in the Middle Triassic.

Sibumasu collision to Indochina-East Malaya is not correlated to the studied intrusions but might triggered plutonisms in Riau Islands and Bangka-Belitong. Meso-Tethys subduction under West Sumatra should have initiated in the Jurassic SAG (Sato, 1991) and the Late Jurassic-Early Cretaceous TGG (Koning and Aulia, 1985 in Barber *et al.,* 2005; Pulunggono and Cameron, 1984). After the closure of the Meso-Tethys, the Indo-Australia Ocean underwent subduction below Sumatra until now and triggered the Cenozoic LaP and LoP (Imtihanah, 2005; Sato, 1991). However, no previous age dating describes the emplacement of the nearshore TP and west Ombilin-situated BP. The emplacement mechanism of studied plutons with their association to Southeast Asia tectonic activities is simplified in Figure 9.

CONCLUSION

Rock samples of seven plutons in central Sumatra were analyzed using petrography and geochemistry

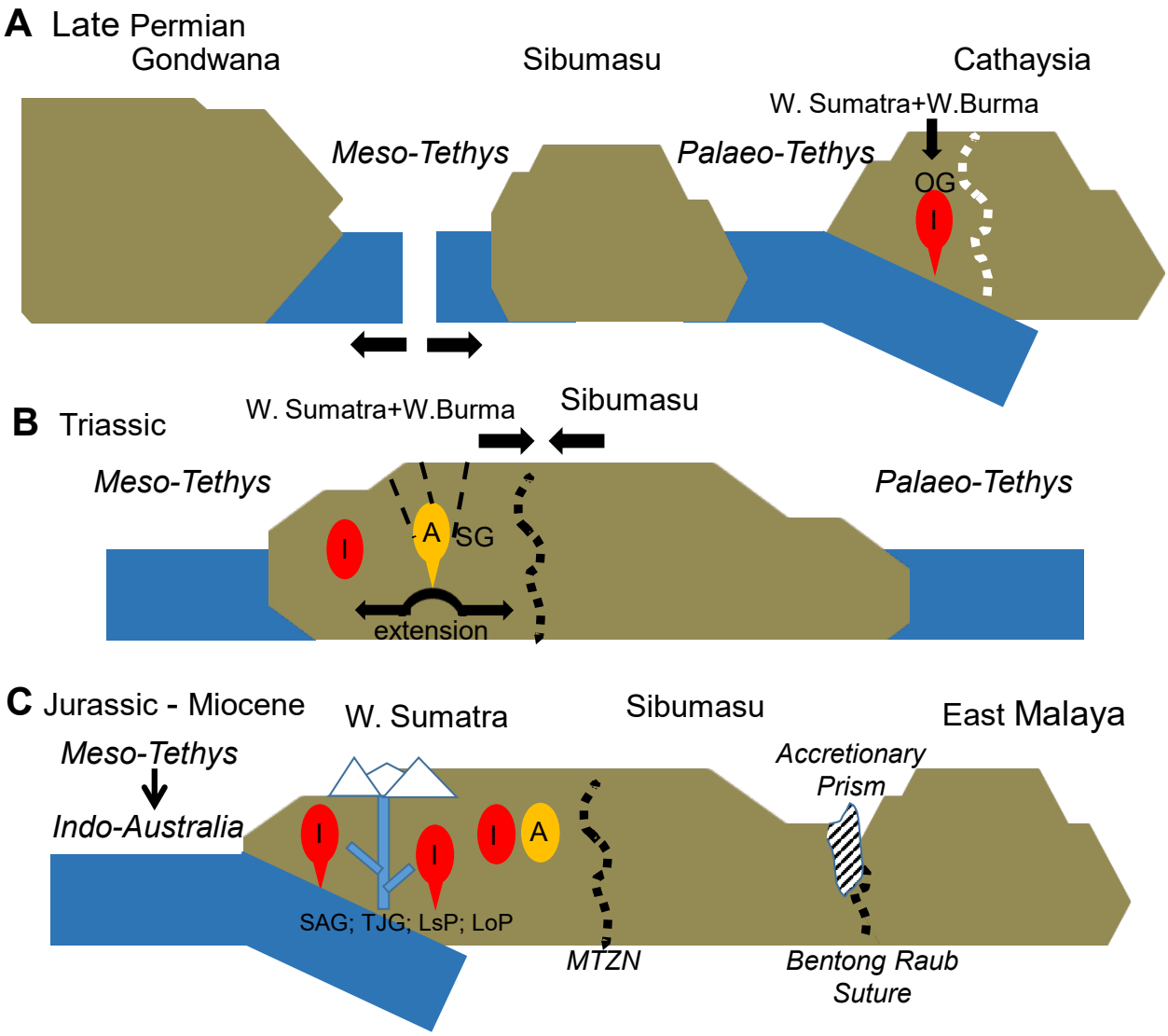

FIGURE 9. Tectonic history in correlation to the studied plutons. A) Ombilin Granite (OG) crystallized because of Palaeo-Tethys subduction before West Sumatra and West Burma separated from Cathaysia; B) the A-type Sinjunjung Granite (SG) was formed due to extension in West Sumatra plate during the Triassic and C) Meso-Tethys subduction below West Sumatra triggered the Sulit Air Granite (SAG) and Tanjung Gadang Granite (TJG) plutonisms. After the closure of Meso-Tethys, Indo-Australia continued the subduction to initiate the Lolo Pluton (LoP) and Lassi Pluton (LaP) crystallizations.

methods. According to their mineral composition, most of the studied plutons in central Sumatra are classified as the I-type intrusions on the presence of biotite-hornblende without muscovite-monazite. A/CNK value <1.1, magnesian affinity, and negative SiO_2-P_2O_5 correlation of the plutons are in line with I-type nature. A-type characters of Sijunjung Granite are amplified from its high SiO_2, Nb, Na_2O+K_2O, and total REE abundances with ferroan and within-plate affinities. The Ombilin Granite should have been formed before the detachment of West Sumatra-West Burma from Cathaysia. The intrusions of Sulit Air Granite and Tanjung Gadang Granite happened due to Meso-Tethys subduction under West Sumatra, whilst the Lassi and Lolo plutons are associated to the Indo-Australia and West Sumatra convergency. The A-type Sijunjung Granites signifies an extensional environment during episodic of subduction in Sumatra.

ACKNOWLEDGMENTS

The authors would like to thank the Head of the Centre for Geological Survey for publicity permission. Professor Hamdan Zainal Abidin contributed with his scientific ideas. The very good laboratory works that were performed by Mrs. Irfanny, Mrs. Indah, and Mrs. Citra are highly acknowledged. Mr. Eko Partoyo, Mr. Baharuddin, and Mr. Heri H. Jazuli helped the

research in petrology point of view. Geochemistry Program in the Center for Geological Survey of Indonesia assisted this research financially.

REFERENCES

Ali, J.R., Aitchison, J.C., 2005. Greater India. Earth-Science Reviews, 72(3-4), 169-188. DOI: 10.1016/j.earscirev.2005.07.005

Amiruddin, A., 2011. Tectonic Rifting of Upper Palaeozoic-Mesozoic Intra-Cratonic Basins in the Southeastern Gondwanaland and Its Economic Aspects. Jurnal Geologi dan Sumberdaya Mineral, 21(5), 249-255.

Barber, A.J., 2000. The origin of the Woyla Terranes in Sumatra and the Late Mesozoic evolution of the Sundaland margin. Journal of Asian Earth Sciences, 18(6), 713-738.

Barber, A.J., Crow, M.J., Milsom, J., (Eds) 2005. Sumatra: Geology, resources and tectonic evolution. London, The Geological Society, 290.

Barber, A.J., Crow, M.J., 2009. Structure of Sumatra and its implications for the tectonic assembly of Southeast Asia and the destruction of Paleotethys. Island Arc, 18(1), 3-20. DOI: 10.1111/j.1440-1738.2008.00631.x

Boynton, W.V., 1984. Cosmochemistry of the rare earth elements: meteorite studies. Developments in Geochemistry, 2, 63-114.

Breitfeld, H.T., Hall, R., Galin, T., Forster, M.A., Boudagher-Fadel, M.K., 2017. A Triassic to Cretaceous Sundaland–Pacific subduction margin in West Sarawak, Borneo. Tectonophysics, 694, 35-56. DOI: 10.1016/j.tecto.2016.11.034

Castro, A., 2020. The dual origin of I-type granites: the contribution from experiments. London, The Geological Society, 491(1, Special Publications), 101-145.

Chappel, B.W., White, A.J.R., 1974. Two contrasting granite types. Pacific geology, 8(2), 173-174.

Chappell, B.W., Bryant, C.J., Wyborn, D., 2012. Peraluminous I-type granites. Lithos, 153, 142-153. DOI: 10.1016/j.lithos.2012.07.008

Charusiri, P., Clark, A.H., Farrar, E., Archibald, D., Charusiri, B., 1993. Granite belts in Thailand: evidence from the 40Ar/39Ar geochronological and geological syntheses. Journal of Southeast Asian Earth Sciences, 8(1-4), 127-136.

Clarke, M.C., Beddoe-Stephens, B., 1987. Geochemistry, mineralogy and plate tectonic setting of a Late Cretaceous Sn-W granite from Sumatra, Indonesia. Mineralogical Magazine, 51(361), 371-387.

Cobbing, E.J., 2005. Granites. London, The Geological Society, 31(1, Memoirs), 54-62.

Cottam, M.A., Hall, R., Sperber, C., Kohn, B.P., Forster, M.A., Batt, G.E., 2013. Neogene rock uplift and erosion in northern Borneo: evidence from the Kinabalu granite, Mount Kinabalu. Journal of the Geological Society, 170(5), 805-816.

Elitok, Ö., Özdamar, Ş., Bacak, G., Uz, B., 2014. Geological, petrological, and geodynamical characteristics of the Karacaali Magmatic Complex (Kırıkkale) in the Central Anatolian Crystalline Complex, Turkey. Turkish Journal of Earth Sciences, 23(6), 645-667. DOI: 10.3906/yer-1312-7

Frost, B.R., Barnes, C.G., Collins, W.J., Arculus, R.J., Ellis, D.J., Frost, C.D., 2001. A geochemical classification for granitic rocks. Journal of petrology, 42(11), 2033-2048.

Frost, C.D., Frost, B.R., Beard, J.S., 2016. On silica-rich granitoids and their eruptive equivalents. American Mineralogist, 101(6), 1268-1284.

Gasparon, M., Varne, R., 1995. Sumatran granitoids and their relationship to Southeast Asian terranes. Tectonophysics, 251(1-4), 277-299.

Gazel, E., Denyer, P., Baumgartner, P.O., 2006. Magmatic and geotectonic significance of santa elena peninsula, costa rica. Geologica Acta, 4(1-2), 193-202.

Ghani, A.A., Searle, M., Robb, L., Chung, S.L., 2013. Transitional IS type characteristic in the main range granite, Peninsular Malaysia. Journal of Asian Earth Sciences, 76, 225-240.

Hall, R., Sevastjanova, I., 2012. Australian crust in Indonesia. Australian Journal of Earth Sciences, 59(6), 827-844. DOI: 10.1080/08120099.2012.692335

Hazad, F.I., Ghani, A.A., Lo, C.H., 2019. Arc related dioritic–granodioritic magmatism from southeastern Peninsular Malaysia and its tectonic implication. Cretaceous Research, 95, 208-224. DOI: 10.1016/j.cretres.2018.10.016

Hutchinson, C.S., 2014. Tectonic evolution of Southeast Asia. Bulletin of the Geological Society of Malaysia, 60, 1-18.

Imtihanah, 2005. Rb/Sr Geochronology and Geochemistry of Granitoid Rocks from Western Part of Central Sumatra. Jurnal Sumber Daya Geologi, 15(2), 103-117.

Irzon, R., Abdullah, B., 2016. Geochemistry of Ophiolite Complex in North Konawe, Southeast Sulawesi. Eksplorium: Buletin Pusat Teknologi Bahan Galian Nuklir, 37(2), 101-114.

Irzon, R., 2017. Geochemistry of Late Triassic weak Peraluminous A-Type Karimun Granite, Karimun Regency, Riau Islands Province. Indonesian Journal on Geoscience, 4(1), 21-37. DOI: 10.17014/ijog.4.1.21-31

Irzon, R., 2018. Comagmatic Andesite and Dacite in Mount Ijo, Kulonprogo: A Geochemistry Perspective. Jurnal Geologi dan Sumberdaya Mineral, 19(4), 221-231.

Irzon, R., Syafri, I., Sendjadja, P., Setiawan, V.E., Hutabarat, J., 2018, September. Rare Earth Elements on the A-type Unggan Granite and Its Comparison to the A-type Section of Sibolga Granite. In Journal of Physics: Conference Series, 1095(1), 012033. DOI: 10.1088/1742-6596/1095/1/012033

Irzon, R., Syafri, I., Ghani, A.A., Prabowo, A., Hutabarat, J., Sendjaja, P., 2020. Petrography and geochemistry of the Pinkish Lagoi Granite, Bintan Island: Implication to magmatic differentiation, classification, and tectonic history. Bulletin of the Geological Society of Malaysia, 69, 27-37. DOI: 10.7186/bgsm69202003

Jamil, A., Ghani, A.A., Zaw, K., Osman, S., Quek, L.X., 2016. Origin and tectonic implications of the ~200 Ma, collision-related Jerai pluton of the Western Granite Belt, Peninsular Malaysia. Journal of Asian Earth Sciences, 127, 32-46.

Jiang, H., Li, W.Q., Jiang, S.Y., Wang, H., Wei, X.P., 2017. Geochronological, geochemical and Sr-Nd-Hf isotopic constraints on the petrogenesis of Late Cretaceous A-type granites from the Sibumasu Block, Southern Myanmar, SE Asia. Lithos, 268, 32-47. DOI: 10.1016/j.lithos.2016.11.005

Kara, J., Väisänen, M., Johansson, Å., Lahaye, Y., O'Brien, H., Eklund, O., 2018. 1.90-1.88 Ga arc magmatism of central Fennoscandia: geochemistry, U-Pb geochronology, Sm-Nd and Lu-Hf isotope systematics of plutonic-volcanic rocks from southern Finland. Geologica Acta, 16(1), 1-23. DOI: 10.1344/GeologicaActa2018.16.1.1

Lee, S.G., Asahara, Y., Tanaka, T., Lee, S.R., Lee, T., 2013. Geochemical significance of the Rb–Sr, La–Ce and Sm–Nd isotope systems in A-type rocks with REE tetrad patterns and negative Eu and Ce anomalies: The Cretaceous Muamsa and Weolaksan granites, South Korea. Geochemistry, 73(1), 75-88. DOI: 10.1016/j.chemer.2012.11.008

Liu, L., Hu, R.Z., Zhong, H., Yang, J.H., Kang, L.F., Zhang, X.C., FU, Y.Z., Mao, W., Tang, Y.W., 2020. Petrogenesis of multistage S-type granites from the Malay Peninsula in the Southeast Asian tin belt and their relationship to Tethyan evolution. Gondwana Research, 84, 20-37 DOI: 10.1016/j.gr.2020.02.013

Loiselle, M.C., Wones, D.R., 1979. Characteristics and origin of anorogenic granites. Geological Society of America, 11, 468.

Maniar, P.D., Piccoli, P.M., 1989. Tectonic discrimination of granitoids. Geological society of America bulletin, 101(5), 635-643.

McCourt, W.J., Crow, M.J., Cobbing, E.J., Amin, T.C., 1996. Mesozoic and Cenozoic plutonic evolution of SE Asia: evidence from Sumatra, Indonesia. London, The Geological Society, 106(1, Special Publications), 321-335.

Metcalfe, I., 2011. Tectonic framework and Phanerozoic evolution of Sundaland. Gondwana Research, 19(1), 3-21. DOI: 10.1016/j.gr.2010.02.016

Metcalfe, I., 2013. Gondwana dispersion and Asian accretion: Tectonic and palaeogeographic evolution of eastern Tethys. Journal of Asian Earth Sciences, 66, 1-33. DOI: 10.1016/j.jseaes.2012.12.020

Middlemost, E.A., 1994. Naming materials in the magma/igneous rock system. Earth-Science Reviews, 37(3-4), 215-224.

Montes, A.D., Vaquero, P.V., Moral, C.R., Garcia, T.S., 2017. Late Variscan, Permo-Carboniferous, Al-K plutonism in the South Portuguese Zone: El Crispinejo cordierite-bearing granite. Geologica Acta, 15(4), 429-442. DOI: 10.1344/GeologicaActa2017.15.4.11

Ng, S.W.P., Whitehouse, M.J., Roselee, M.H., Teschner, C., Murtadha, S., Oliver, G.J., Ghani, A.A., Chang, S.C., 2017. Late triassic granites from Bangka, Indonesia: A continuation of the main range granite province of the South-East Asian tin belt. Journal of Asian Earth Sciences, 138, 548-561. DOI: 10.1016/j.jseaes.2017.03.002

Nguyen, T.A., Yang, X., Thi, H.V., Liu, L., Lee, I., 2019. Piaoac granites related W-Sn mineralization, Northern Vietnam: evidences from geochemistry, zircon geochronology and Hf isotopes. Journal of Earth Science, 30(1), 52-69.

Patiño Douce, A.E., 1997. Generation of metaluminous A-type granites by low-pressure melting of calc-alkaline granitoids. Geology, 25(8), 743-746.

Pearce, J.A., Harris, N.B., Tindle, A.G., 1984. Trace element discrimination diagrams for the tectonic interpretation of granitic rocks. Journal of petrology, 25(4), 956-983.

Peccerillo, A., Taylor, S.R., 1976. Geochemistry of Eocene calc-alkaline volcanic rocks from the Kastamonu area, northern Turkey. Contributions to mineralogy and petrology, 58(1), 63-81.

Pérez-Soba, C., Villaseca, C., 2010. Petrogenesis of highly fractionated I-type peraluminous granites: La Pedriza pluton (Spanish Central System). Geologica Acta, 8(2), 131-149. DOI: 10.1344/105.000001527

Pollard, P.J., Nakapadungrat, S., Taylor, R.G., 1995. The Phuket Supersuite, Southwest Thailand; fractionated I-type granites associated with tin-tantalum mineralization. Economic Geology, 90(3), 586-602.

Pulunggono, A., Cameron, N.R., 1984. Sumatran microplates, their characteristics and their role in the evolution of the Central and South Sumatra basins. Indonesian Petroleum Association, Proceedings of the Annual Convention-Indonesian Petroleum Association, 1, 121.

Rosidi, H.M.D., Tjokrosapoetro, S., Pendowo, B., Gafoer, S., 1996. The Geology of the Painan and Northeastern Part of the Muarasiberut, Quadrangles (0814-0714), Systematic Geological Map of Indonesia Scale 1: 250000.

Sarjoughian, F., Kananian, A., 2017. Zircon U-Pb geochronology and emplacement history of intrusive rocks in the Ardestan section, central Iran. Geologica Acta, 15(1), 25-36. DOI: 10.1344/GeologicaActa2017.15.1.3

Sato, K., 1991. K-Ar ages of granitoids in Central Sumatra, Indonesia. Bulletin Geological Survey of Japan, 42, 111-181.

Searle, M.P., Whitehouse, M.J., Robb, L.J., Ghani, A.A., Hutchison, C.S., Sone, M., Ng, S.P., Roselee, M.H., Chung, S.L., Oliver, G.J.H., 2012. Tectonic evolution of the Sibumasu–Indochina terrane collision zone in Thailand and Malaysia: constraints from new U–Pb zircon chronology of SE Asian tin granitoids. Journal of the Geological Society, 169(4), 489-500.

Setiawan, I., Takahashi, R., Imai, A., 2017. Petrochemistry of granitoids in Sibolga and its surrounding areas, North Sumatra, Indonesia. Resource Geology, 67(3), 254-278. DOI: 10.1111/rge.12132

Silitonga, P.H., Kastowo, D., 1995. Geological Map of the Solok Quadrangle, Sumatra (Quadrangle 0815) Scale 1: 250,000. Geological Research and Development Centre Bandung.

Stammeier, J., Jung, S., Romer, R.L., Berndt, J., Garbe-Schönberg, D., 2015. Petrology of ferroan alkali-calcic granites: Synorogenic high-temperature melting of undepleted felsic lower crust (Damara orogen, Namibia). Lithos, 224, 114-125. DOI: 10.1016/j.lithos.2015.03.004

Streckeisen, A., 1976. To each plutonic rock its proper name. Earth-science reviews, 12(1), 1-33.

Sun, S.S., McDonough, W.F., 1989. Chemical and isotopic systematics of oceanic basalts: implications for mantle composition and processes. London, The Geological Society, 42(1, Special Publication), 313-345.

Sutanto, 2005. Distribusi, Mineralogi, dan Komposisi Kimia Granitoid di Sumatra. Jurnal Wahana Teknik, 7(1), 1-14.

Whalen, J.B., Currie, K.L., Chappell, B.W., 1987. A-type granites: geochemical characteristics, discrimination and petrogenesis. Contributions to mineralogy and petrology, 95(4), 407-419. DOI: 10.1007/BF00402202

White, A.J.R., Chappell, B.W., 1983. Granitoid types and their distribution in the Lachlan Fold Belt, southeastern Australia. Geological Society of America Memoir, 159(12), 21-34.

Zhang, X., Chung, S.L., Lai, Y.M., Ghani, A.A., Murtadha, S., Lee, H.Y., Hsu, C.C., 2018. Detrital Zircons Dismember Sibumasu in East Gondwana. Journal of Geophysical Research: Solid Earth, 123(7), 6098-6110. DOI: 10.1029/2018JB015780

Zhang, H., Hu, P., Cao, L., Tampubolon, A., Liu, A., Cheng, X., Zhan, M., Pan, L., Dai, Y., Pan, B., 2020. Geochemical characteristics and Sr-Nd-Hf isotope compositions of Late Triassic post-collisional A-type granites in Sarudik, SW Sumatra, Indonesia. Island Arc, 29(1), p.e12357.

Manuscript received September 2020;
revision accepted May 2021;
published Online July 2021.

APPENDIX I

TABLE I. Major oxides composition of intrusive rocks from seven plutons in Central Sumatra

Sample	SiO_2	TiO_2	Al_2O_3	Fe_2O_{3T}	MgO	MnO	CaO	Na_2O	K_2O	P_2O_5	LOI
Lassi Pluton											
LS-16	55.70	0.46	21.80	4.90	2.84	0.14	6.18	4.17	1.05	0.38	2.11
LS-17	61.58	0.31	19.12	4.24	2.45	0.15	6.47	3.08	1.12	0.32	0.97
LS-15	60.63	0.43	17.88	3.83	1.16	0.11	4.28	3.45	2.88	0.15	4.81
LS-62	61.84	0.59	18.01	4.79	2.60	0.10	4.36	3.54	3.04	0.15	0.79
LS-63	61.68	0.63	18.09	4.76	2.81	0.10	4.21	3.32	3.53	0.15	0.49
SM 27 A[1]	66.82	0.31	17.58	2.5	0.44	0.06	3.62	5.89	1.40	0.08	1.08
I 98/01[2]	75.09	0.17	13.83	1.09	0.22	0.03	0.63	4.11	4.39	0.04	0.37
I 98/02[2]	69.77	0.21	17.22	2.31	0.64	0.06	3.92	4.58	1.20	0.09	0.34
I 98/03[2]	50.62	0.95	17.87	11.96	4.73	0.20	9.27	3.20	1.10	0.11	1.06
I 98/04[2]	63.98	0.42	17.27	5.42	1.92	0.13	5.82	3.79	0.80	0.24	1.29
S4[3]	79.2	0.13	12.15	1.2	0.31	0.04	1.35	3.95	1.06	0.02	0.74
PD 5[3]	53.6	1.10	19.1	9.00	2.95	0.19	6.6	4.50	1.51	0.63	0.63
Sijunjung Granite											
SJ-30	68.50	0.26	17.10	2.32	0.46	0.04	0.88	3.59	5.45	0.10	1.50
SJ-31	68.80	0.34	16.30	2.90	0.59	0.04	1.60	3.24	4.91	0.12	0.98
SJ-87	70.75	0.34	13.51	3.76	0.43	0.05	1.78	2.95	5.49	0.12	0.77
SJ-89	66.05	0.42	17.32	4.23	0.37	0.05	0.71	2.31	4.94	0.05	3.01
SJ-90	71.46	0.18	14.18	2.68	0.16	0.04	1.01	3.02	5.86	0.07	1.01
SB43[1]	72.71	0.32	14.05	2.17	0.29	0.06	1.21	3.24	5.12	0.19	0.7
RD 16[3]	69	0.4	14.70	2.52	0.61	0.06	2.17	3.12	5.62	0.12	0.35
SB-90 B	71.46	0.18	14.18	2.68	0.163	0.04	1.01	3.02	5.86	0.07	1.01
Sulit Air Suite											
SA-34	56.46	0.68	18.97	6.48	4.22	0.13	6.67	2.97	2.25	0.27	0.66
SA-54	60.59	0.48	17.84	5.33	3.39	0.11	5.06	3.05	2.58	0.16	1.23
I 98/07[2]	63.18	0.52	16.24	6.24	2.73	0.10	5.54	3.22	2.32	0.10	1.5
I 98/08[2]	63.85	0.51	16.07	5.93	2.52	0.12	5.44	3.28	2.18	0.12	1.51
Ombilin Granit											
OB-26	64.37	0.38	18.18	3.00	2.42	0.08	3.72	3.63	3.15	0.19	0.72
OB-27	61.47	0.20	21.41	2.61	1.72	0.06	3.90	4.41	1.95	0.16	1.93
Tarusan Pluton											
TR-35 A	71.77	0.12	15.46	1.02	0.21	0.01	1.56	4.50	4.69	0.01	0.84
TR 35-B	70.79	0.09	16.51	0.95	0.23	0.00	1.63	5.14	3.68	0.00	1.19
Lolo Pluton											
LL-59	68.44	0.31	16.07	3.00	1.36	0.05	3.21	3.88	3.23	0.10	0.51
LL-58 A	50.57	1.03	18.11	10.55	4.90	0.11	7.70	5.63	0.48	0.15	0.64
LL-58 B	72.39	0.14	16.50	0.58	0.15	0.01	1.13	3.36	4.95	0.05	0.63
I-98-9[2]	71.55	0.33	14.10	3.23	0.87	0.054	2.87	3.52	3.06	0.066	0.39
I-98-10[2]	65.88	0.58	16.13	4.78	1.66	0.097	4.46	3.57	2.65	0.14	0.59
I-98-11[2]	64.79	0.55	16.07	5.64	2.03	0.092	5.36	3.55	1.97	0.1	0.48
I-98-13[2]	74.91	0.18	13.54	1.63	0.35	0.027	1.61	3.28	4.3	0.03	0.39
Tanjung Gadang Granite											
TG-05	69.27	0.26	16.26	2.65	0.94	0.07	1.68	4.13	3.22	0.08	1.27

TABLE II. Trace and rare earth elements abundance. 1: Sato (1991), 2: Imtihanah (2005) and 3: Sutanto (2005)

Sample	Sc	Ga	Rb	Sr	Y	Ba	La	Ce	Pr	Nd	Sm	Eu	Gd	Tb	Dy	Ho	Er	Tm	Yb	Lu
Lassi Pluton																				
LS-16	10.35	11.97	25	800	9.44	332.2	10.29	8.07	2.45	10.52	2.26	0.74	0.88	0.23	1.62	0.31	0.89	0.15	0.84	0.11
LS-17	6.52	9.80	24	589	7.08	373	11.6	9.08	2.67	10.7	1.96	0.61	0.79	0.18	1.27	0.24	0.67	0.14	0.68	0.1
LS-15	7.86	9.18	78	204	18.4	436	15.3	11.3	3.48	14.2	3.07	0.71	1.28	0.34	2.59	0.51	1.5	0.21	1.47	0.2
LS-62	12.03	12.52	95	171	34.24	409	28.96	26.41	7.65	33.76	8.14	1.14	3.44	1.13	9.9	2.05	6.39	0.9	6.79	0.72
LS-63	9.93	11.40	121	164	28.5	443	24.2	22.7	6.81	30.1	7.2	1.04	3.05	1.02	8.57	1.76	5.38	0.77	5.66	0.61
I 98/02[2]	3.60	17.70	26.9	1062	4.5	548	20.6	35.6	n.a.	13.6	n.a.	n.a.	n.a.	n.a.	n.a.	n.a.	n.a.	n.a.	n.a.	n.a.
I 98/03[2]	38.5	18.20	21.2	649	16.5	409	6.4	17.6	n.a.	9.4	n.a.	n.a.	n.a.	n.a.	n.a.	n.a.	n.a.	n.a.	n.a.	n.a.
I 98/04[2]	15.8	18.30	19.6	850	10.7	627	17	33.5	n.a.	16.1	n.a.	n.a.	n.a.	n.a.	n.a.	n.a.	n.a.	n.a.	n.a.	n.a.
S4[3]	2.00	n.a.	22	335	5	530	50	77	n.a.	24	n.a.	1	n.a.	n.a.	0.9	n.a.	0.6	n.a.	0.42	n.a.
PD 5[3]	20.00	n.a.	37	720	39	875	27	57	n.a.	38	n.a.	1.95	n.a.	n.a.	6.6	n.a.	3.6	n.a.	3	n.a.
Sijunjung Granite																				
SJ-30	3.86	37.00	394	125	233	676	435	94.6	106	401	88.9	6.37	32.5	10.7	82.5	15	42.8	5.8	44	4.26
SJ-31	4.42	25.30	252	184	34.8	615	105	80.7	22.9	89	17	1.88	6.62	1.74	12.8	2.36	6.84	0.92	6.72	0.67
SJ-87	3.80	17.64	270	149.9	25.15	496.3	39.78	76.89	9.41	31.96	6.03	0.93	4.79	0.71	5.42	0.83	2.22	0.29	2.54	0.27
SJ-89	4.35	19.93	297	111.2	32.09	778.6	53.75	113	12.78	43.2	7.95	1.14	6.24	0.82	6.48	0.97	2.71	0.32	3.33	0.3
SJ-90	2.41	18.64	429	76	54.55	347.1	36.43	50.89	10.58	37.05	8.28	0.86	5.77	0.92	8.79	1.38	4.72	0.48	7.21	0.48
RD 16[3]	8.00	n.a.	230	210	40	1065	45	90	n.a.	43	n.a.	1.61	n.a.	n.a.	n.a.	n.a.	n.a.	n.a.	n.a.	n.a.
SB-90 B[3]	2.41	18.64	429	76	54.55	347.1	36.43	50.89	10.58	37.05	8.28	0.86	5.77	0.92	8.79	1.38	4.72	0.48	7.21	0.48
Sulit Air Suite																				
SA-34	20.23	15.47	73	353	29.03	424.8	26.58	25.94	8.2	38.32	9.19	1.65	3.76	1.13	9.19	1.86	5.66	0.79	5.96	0.64
SA-54	15.6	11.90	75	278	26.4	530	15.7	15.2	4.63	21.8	5.75	1.02	2.52	0.86	7.58	1.63	5.03	0.73	5.47	0.61
I 98/07[2]	28.00	14.40	62.1	344	22.5	418	8.7	23.1	n.a.	13.4	n.a.	n.a.	n.a.	n.a.	n.a.	n.a.	n.a.	n.a.	n.a.	n.a.
I 98/08[2]	22.40	15.00	56.9	343	26.6	400	9.9	2.6	n.a.	14.3	n.a.	n.a.	n.a.	n.a.	n.a.	n.a.	n.a.	n.a.	n.a.	n.a.

TABLE II. Continued.

Sample	Sc	Ga	Rb	Sr	Y	Ba	La	Ce	Pr	Nd	Sm	Eu	Gd	Tb	Dy	Ho	Er	Tm	Yb	Lu
Ombilin Granite																				
OB-26	3.13	8.73	83	64.4	11.6	535	24.4	21	5.52	23	4.56	0.91	1.98	0.51	3.77	0.75	2.32	0.33	2.57	0.28
OB-27	8.06	15.70	94	407	23.3	781	40.4	30.4	9.6	39.4	8.37	1.88	3.57	1.06	8.39	1.64	5.03	0.75	5.91	0.62
Tarusan Pluton																				
TR-35 A	1.94	19.40	122	61	25	279	34.02	56.45	7.75	26.97	3.28	0.02	2.82	0.55	1.58	0.45	0.61	0.26	1.4	0.18
TR 35-B	2.08	16.40	90	79	19.2	189	8.94	21.4	1.6	5.55	0.3	0.01	0.21	0.24	0.42	0.29	0.25	0.23	1.29	0.17
Lolo Pluton																				
LL-59	2.92	7.82	113	106	11.97	435	7.85	17.5	1.54	6.25	0.58	0.22	0.31	0.33	1	0.38	0.43	0.23	1.13	0.13
LL-58 A	2.57	13.30	25	126	24.4	555	28.7	25.7	7.66	32.7	7.41	0.96	2.9	0.93	7.49	1.48	4.52	0.65	4.92	0.52
LL-58 B	5.78	20.80	28	131	32.5	512	75.4	64	20.5	85	17.1	1.41	5.84	1.57	11.2	2.05	6.05	0.84	6.42	0.69
I-98-9[2]	10.60	13.90	97.7	10.60	21.3	165	21.3	3.5	n.a.	12.8	n.a.	n.a.	n.a.	n.a.	n.a.	n.a.	n.a.	n.a.	n.a.	n.a.
I-98-10[2]	14.20	16.70	10.8	14.20	27	283	27	6.4	n.a.	20.8	n.a.	n.a.	n.a.	n.a.	n.a.	n.a.	n.a.	n.a.	n.a.	n.a.
I-98-11[2]	21.00	16.60	62.7	210	27	257	27	3.2	n.a.	13.5	n.a.	n.a.	n.a.	n.a.	n.a.	n.a.	n.a.	n.a.	n.a.	n.a.
I-98-13[2]	4.20	12.60	138.8	4.20	19.2	117	19.2	4.8	n.a.	13.7	n.a.	n.a.	n.a.	n.a.	n.a.	n.a.	n.a.	n.a.	n.a.	n.a.
Tanjung Gadang Granite																				
TG-05	12.21	12.49	109	174	88.52	567.5	32.88	19.04	8.25	35.28	9.36	1.56	4.39	1.55	13.48	2.75	8.26	1.13	7.98	1.06